Effect of the MHD Perturbations on Runaway Beam Formation during Disruptions in the T-10 Tokamak

P. V. Savrukhin 1), E. V. Popova 1), A. V. Sushkov 1), D. E. Kravtsov 1), S. A. Grashin 1),
V. P. Budaev 1), D. P. Ivanov 1), P. D. Ivanov 1), L. N. Khimchenko 1), S. G. Maltsev 1), Y.
D. Pavlov 1), D. V. Sarychev 1), and the T-10 Group

1) Russian Research Center "Kurchatov Institute", 123182, Moscow, Russia

e-mail contact of main author: psavrukhin@bk.ru

ABSTRACT. Repetitive bursts of the non-thermal x-ray (E~100 keV) radiation are observed during plasma current decay phase of the density limit disruptions in the T-10 tokamak. Analysis indicated that the phenomena can be connected with the nonthermal electrons initiated during magnetic flux reconnection in series of minor disruptions. Application of the electron cyclotron waves allows delaying and in some cases preventing formation of the nonthermal beams. Analysis indicated that prevention of the nonthermal beams can be connected with elimination of the bursting MHD modes and reduction of the longitudinal electric field during auxiliary plasma heating.

1. Introduction

Acceleration of electrons to high energies (up to 3-30MeV) during disruption instability is a major concern for future tokamak reactors [1]. The disruption-generated high energy (runaway) electrons can produce several detrimental effects, including damage of the plasma facing components, large electromagnetic loads on conducting structures due to induced currents, and sudden thermal loads on divertor surfaces. In spite of the fact that several techniques (gas jet and pellet injection, see [1], resonant magnetic perturbations [2]) are successfully used for mitigation of the runaway beams in present day tokamaks, direct extrapolation of the techniques for tokamak reactors is complicated. Prediction of the runaway generation and design of reliable techniques for the beams mitigation are considered among important issues for operation of tokamak reactor.

The electron acceleration is generally connected with enhanced longitudinal electric fields (E_0 ~ 2-5 V/m) formed in the cooled post disruption plasma (see [1]). The process is typically described by the primarily Dreicer mechanism with subsequent avalanche formation, while dominant losses of the beams are generally connected with turbulent diffusion due to the magnetohydrodynamic (MHD) modes (see Fig.1). Generation of the powerful runaway beams depends critically on amplitude of the longitudinal electric field and parameters of the background plasma (e.g., electron temperature, T_e, and density, n_e). The high temperature plasma with low density as well as plasma with strong longitudinal electric field after an energy quench during disruption instability is especially favourable for the runaway beam formation. Moreover, beams generation is facilitated in presence of the initial ("seed") population of the nonthermal electrons. Such "seed" nonthermal population can be presented in some cases (e.g. during powerful auxiliary heating) in pre-disruption plasma or can be initiated due to strong electric fields (E_1~10-50V/m) during magnetic reconnection at the initial stage of the disruption [3].

Present study evaluates possible role of the localised nonthermal electrons induced during bursting MHD modes with subsequent formation of the powerful runaway beams in high-density limit disruption and considers possible delay of the beams formation by control the MHD modes using electron cyclotron resonant heating (ECRH).
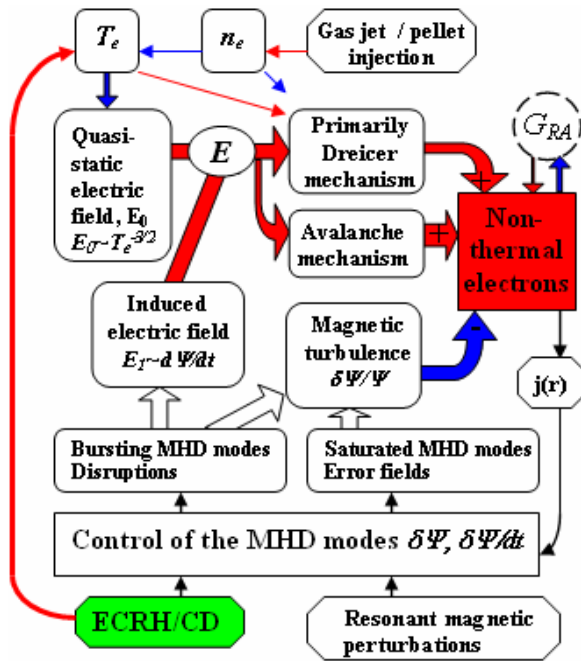
FIG. 1. Schematic view of the mechanisms leading to generation of the non-thermal electron beams in a tokamak plasma. Growth of the MHD modes and subsequent reconnection of the magnetic fluxes around the resonant magnetic surfaces can induce strong electric fields $E_1 >> E_0$, which can facilitate production of the localized beams of the non-thermal electrons, here E_0 is "equilibrium" longitudinal electric field. Control of the MHD modes using ECRH and Resonant Magnetic Perturbation can delay (suppress) production of the runaway beams. Plasma heating during ECRH can lead to decrease of the "equilibrium" electric field and subsequent reduction of the runaway beams.

2. Experimental setup and diagnostics.

The nonthermal x-ray bursts accompanying large-scale MHD modes during density limit disruptions were studied in the T-10 tokamak (major and minor radii, $R_0 = 1.5\ m$, $a_L = 0.28 - 0.3\ m$, accordingly, toroidal magnetic field, $B_t = 1.6 - 2.4\ T$, plasma current, $I_p = 0.2 - 0.33\ MA$). In order to distinguish nonthermal bursts in the T-10 tokamak from previously analysed instabilities induced by intensive electron beams in nonthermal plasma (formed in discharges with low density, powerful auxiliary heating, and, in particular, during non-inductive current drive) present experiments considers plasma with relatively high electron density [central line-averaged density $<n_e>$ up to $\sim (4.5-5.0)\ 10^{19}\ m^{-3}$].

The nonthermal bursts are analysed with the use of a toroidally viewing x-ray array [3], standard x-ray tomographic systems [4] and x-ray gas detectors [5] (see Fig. 2). Additional *NaI(Tl)* monitor (placed outside the tokamak vessel) is used for measurements of the nonthermal ($E_\gamma \sim 0.5\text{-}3\ MeV$) x-ray and neutrons radiation.

Tangential x-ray array (*TX - array*) is placed inside the tokamak vacuum vessel at the low field side of the torus bellow the equatorial midplane [see (1) in Fig. 2]. The system consists of the Si and CdTe x-ray detectors with Soller collimators placed inside protection container at the top of the movable rod. The detectors provide measurements of the emissivity fluxes in energy range ($E_\gamma \sim 2.5\text{- }200\ keV$) with spatial and time resolution of order of $\delta r \sim 7\ mm$ and $3\ \mu s$, accordingly.

The radiation power is measured using in-vessel silicon AXUV-photodiode (Absolute eXtreme UltraViolet) detectors. AXUV-photodiode detectors permit absolute radiated power measurements over range in photon energies $1eV < E < 6000$ eV with the nearly constant conversion efficiency (0.25 A/W) somewhat reduced in the region $1eV<Eph<30$ eV [6]. The diagnostic system consists of array of the 16 AXUV-photodiodes placed below the equatorial midplane. The field of view provides full plasma cross-section coverage (-30 cm ÷30 cm) with spatial resolution of order of 4cm at the vessel midplane. Temporal resolution of the system is 8 μs.

Auxiliary heating (ECRH) system in T-10 consists of five gyrotrons with a total heating power of up to 2.5MW: 1.2MW at 130 GHz and 1.3MWat 140 GHz. An extraordinary wave on the 2nd ECR harmonic is launched from the low field side (LFS) in the direction of the major radius. The width of the ECRH power absorption profile is ≈2% of the minor radius, power density up to 25Wcm−3 is achievable. The cut-off densities are $n_{cut-off}$(140 GHz) ~ 1.2 × 10^{20} m^{-3} and $n_{cut-off}$(130 GHz) ~ 1 × 10^{20} m^{-3}.
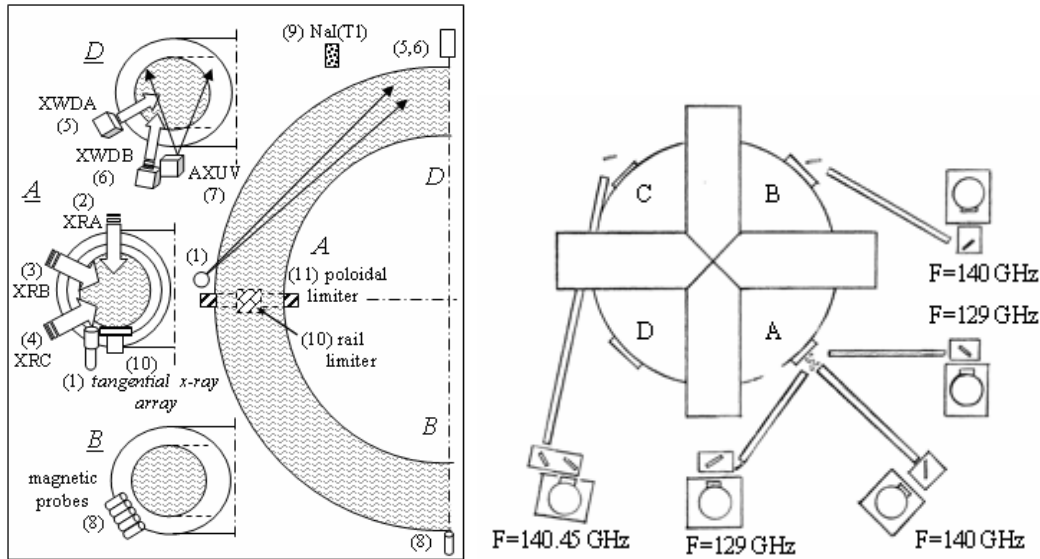

FIG. 2 Schematic view of the diagnostics in the T-10 tokamak. Nonthermal x-ray bursts and MHD modes are analysed by means of the tangential x-ray array, TX (1), standard x-ray tomographic arrays XRA (2), XRB (3), XRC (4), x-ray gas detectors XWDA, XWDB (5,6). Also shown are AXUV detectors (7), fast magnetic probes (8), and NaI(Tl) monitor (9). Plasma in T-10 is restrained by a movable rail limiter (10) and guard poloidal limiter (11). Auxiliary heating (ECRH) system in T-10 consists of five gyrotrons with a total heating power of up to 2.5MW: 1.2MW at 130 GHz and 1.3MWat 140 GHz.

3. Experimental results

The non-thermal x-ray perturbations are initially studied during the density limit disruptions in ohmically heated plasma. The evolution of the plasma parameters in the experiment is shown in Fig. 3. Similarly to a "classical" disruptions observed in tokamaks at high density (see [1,7]), additional gas puff at the quasi-stationary stage of discharge (see, *t > 650 ms* in Fig. 3) is accompanied by increase of the total radiated power and intensive cooling of the plasma edge. Subsequent erosion of the electron temperature profile outside the *q=2* surface leads to formation of an unstable plasma configuration with explosive growth of the MHD perturbations and rapid loss of the stored plasma energy during an energy quench (see mark T1 at *t~745 ms* in Fig. 3). Tomographic analysis of the x-ray emissivity measured using conventional x-ray arrays (*XRA, XRB, XRC*) indicated that energy quench is proceeded by joint rotation of the coupled *m=1, n=1* and *m=2, n=1* perturbations (see detailed analysis of the process in [4]). The disruption is continued with decay of the plasma current, I_p, accompanied with strong increase of the loop voltage, U_l.

The first minor disruption (see mark T1 at *t~745 ms* in Fig. 3) is also accompanied by bursts of the hard x-ray emission, I_{HXR} and spike of the nonthermal radiation observed using

conventional (*xra15*) and tangentially viewing x-ray arrays (*txray3*). Analysis indicated that the first spike during density limit disruption is connected with interaction of the nonthermal electrons with the rail limiter (see [8]). While the spikes are observed in virtually all disruptions under study, their amplitude can be changed considerably in various plasma conditions. Amplitude of the non-thermal x-ray spikes at the first minor disruption can be reduced up to 5-15 times in plasma with strong gas puffing. Intensive spikes of the x-ray radiation are generally observed during an energy quench in plasma with relatively high density and slow rate of the gas puff.
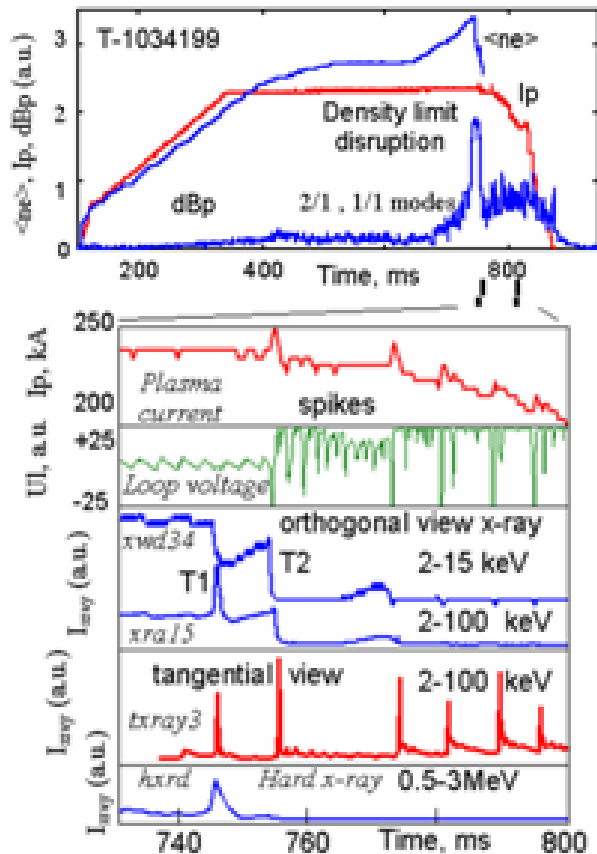

FIG. 3. Time evolution of the plasma parameters during density limit disruption in the T-10 tokamak. Here, Ip -plasma current, dBp - magnetic field perturbations, <ne> - plasma density, Ul -loop voltage. Also shown, are x-ray intensity measured using gas detector and CdTe detectors with orthogonal view of the plasma column (xwd34 and xra15, accordingly), x-ray intensity measured using tangential view CdTe detector txray3 and hard x-ray intensity, hxrd, measured using NaI(Tl) monitor. Repetitive bursts of the non-thermal x-ray radiation (txray3) from the plasma core indicate periodic generation of the nonthermal electrons in series of minor disruptions

Intensive x-ray bursts during energy quench at disruptions at high density [1] (as well as disruptions at high β [10]) were described previously [9,11]. Essential new part of the present studies is observation of the phenomenologically similar x-ray bursts during decay of the plasma current. The bursts are observed in the case most clearly using tangentially viewing x-ray arrays (see *txray3* in Fig.3) and are not observed with conventional view x-ray arrays with orthogonal view of the plasma column (see *xra15 and xwd34* in Fig.3). This indicates indirectly, that the bursts are connected with bremsstrahlung x-ray radiation from the nonthermal electrons in flight. Analysis indicates that soft x-ray radiation observed with the conventional x-ray arrays after the energy quench is confined within the plasma core (see Fig.4a). The x-ray perturbations are localised around the same area as one of the "giant" m=1,n=1 helical perturbations [4] observed just after the energy quench (see Fig.4a). Intensive radiation bursts during the plasma current decay are observed also with the AXUV detectors (see Fig.4b).

Phenomenologically similar evolution of the bursts after an energy quench is observed in T-10 in various plasma conditions (e.g. various toroidal magnetic fields, B_t=1.6-2.4T, plasma current, Ip=0.15-0.3MA) during gas puff and pellet injection and during experiments with

ramp up of the plasma current. ECRH heating at moderate power (Pec~1.3MW, 140GHz) does not change considerably evolution of the bursts (see Fig.5), while soft x-ray intensity from the plasma core is increased in the case.
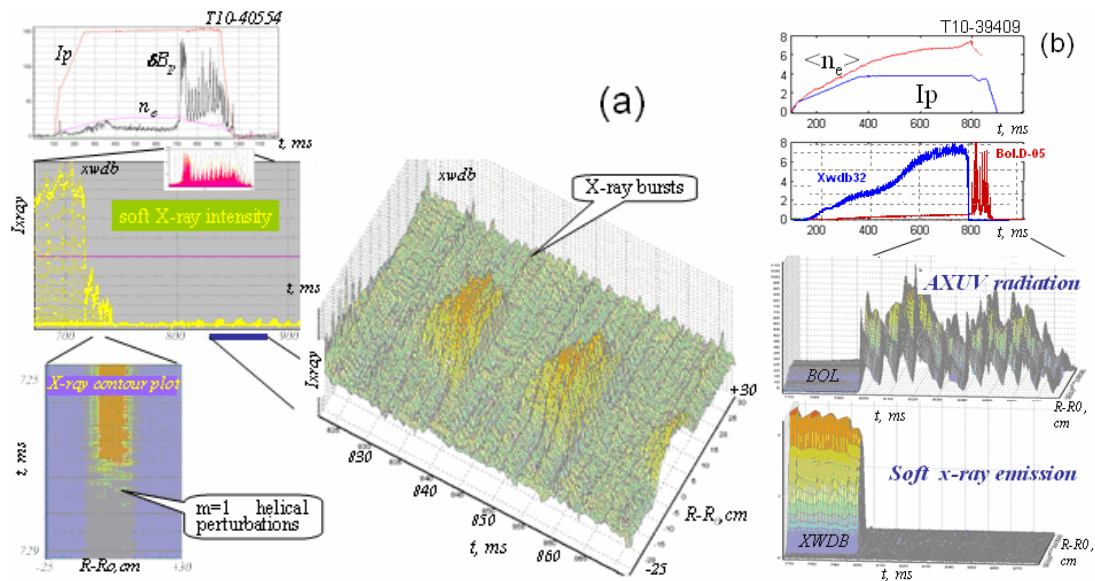

FIG. 4 (a) Time evolution of the plasma current Ip, magnetic field perturbations dBp, plasma density ne, and soft x-ray intensity measured using gas detector with orthogonal view of the plasma column xwdb. Also shown are contour plots of the x-ray intensity measured just after energy quench at the density limit disruption and during series of the x-ray burst. (b) Time evolution of the plasma current Ip, plasma density ne, soft x-ray intensity measured using gas detector XWDB, and total radiation power measured using AXUV detector (BOL). Also shown are contour plots of the x-ray intensity (XWDB) and total radiation power (AXUV) measured after energy quench at the density limit disruption.
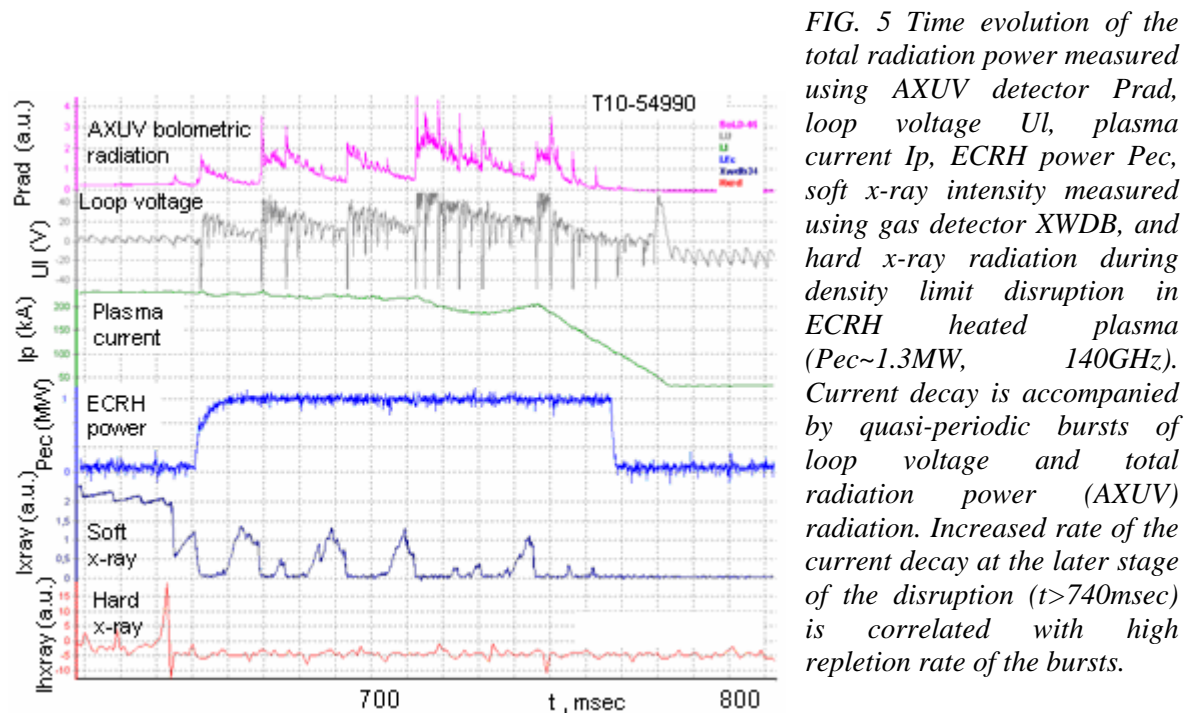

FIG. 5 Time evolution of the total radiation power measured using AXUV detector Prad, loop voltage Ul, plasma current Ip, ECRH power Pec, soft x-ray intensity measured using gas detector XWDB, and hard x-ray radiation during density limit disruption in ECRH heated plasma (Pec~1.3MW, 140GHz). Current decay is accompanied by quasi-periodic bursts of loop voltage and total radiation power (AXUV) radiation. Increased rate of the current decay at the later stage of the disruption (t>740msec) is correlated with high repletion rate of the bursts.

Quasi-periodic bursts of the nonthermal x-ray and total radiation power (AXUV) is correlated with negative spikes of the loop voltage and temporal increases of the plasma current (see Fig.3 and Fig.5). Such behavior of loop voltage and plasma current is typical for major disruptions and are generally associated with partial reconnection of the poloidal magnetic flux [1,7]. This can indicate indirectly that spikes of the nonthermal x-ray radiation can be connected with nonthermal electrons induced due to the bursting electric fields at the "reconnection events" [3,7].

Current decay rate is clearly correlates with repletion rate of the quasi-periodic bursts of loop voltage, nonthermal x-ray and total radiation power (AXUV). Increased rate of the current decay at the later stage of the disruption (t ~ 715 – 730 msec and t ~ 745 - 770 msec in Fig.5) is correlated with high repletion rate of the bursts.

ECRH allows control of the MHD modes and removal of the nonthermal x-ray and total radiation power (AXUV). Typical time evolution of the plasma parameters is shown in the case in Fig.6. ECRH power is switched on at t=625msec (5 msec after the energy quench). Radiation due to the nonthermal electrons is removed for the whole duration of the ECRH pulse and plasma current is sustained. Essential feature of the experiments is elimination of the bursting MHD modes and disappearance of the loop voltage spikes. This effect is observed at relatively high ECRH power (operation of all five gyrotrons with a total heating power of up to 2.5MW: 1.2MW at 130 GHz and 1.3MWat 140 GHz is required in the case).

3. Discussion and Conclusions

Repetitive bursts of the non-thermal x-ray (E~100 keV) and total radiation (AXUV) observed during plasma current decay phase of the density limit disruptions in the T-10 tokamak can indicate possible connection of the phenomena with the nonthermal electrons. While present experiments can not provide detailed information for quantitative analysis of the process, it seems that spikes in loop voltage during current decay phase of the disruption indicated that nonthermal electrons can be in fact initiated during reconnection in series of minor disruptions. Experimental observations are confirmed indirectly by numerical modelling (see detailed description of the model in [8]) indicating that periodic growth of the helical electric field during magnetic reconnection at the minor disruptions can considerably increase the runaway beam production (Fig.7a). Generation of the nonthermal electrons is suppressed considerably with increase on the magnetic field perturbations (Fig.7c). This effect (in addition to the standard runaway acceleration in the longitudinal electric field) has indicated that control of the MHD modes may be required for the runaway suppression.

Application of the electron cyclotron waves allows delaying and in some cases preventing formation of the primarily runaway beams. Analysis indicated that prevention of the runaway beams can be connected with elimination of the bursting MHD modes and reduction of the longitudinal electric field during auxiliary plasma heating. Results of numerical modeling of the runaway beams in the T-10 plasma with auxiliary heating are shown in Fig.7d. In agreement with experiments, numerical modelling indicates decay of the runaway beams during auxiliary plasma heating after increase of the electron temperature and subsequent reduction of the "longitudinal" electric field.

In conclusion, bursts of the nonthermal x-ray intensity and radiation is observed in T-10 plasma during current decay stage of the density limit disruptions. Analysis indicted that bursts can be connected with nonthermal electrons generated during magnetic reconnection in series of minor disruptions. Accordingly with results of numerical modelling such periodic

generation of the nonthermal electrons can facilitate production of the powerful runaway beams. Application of the ECRH heating allows delaying and in some cases preventing generation of the primarily nonthermal electrons. Numerical modelling indicted that this effect can be connected with heating of the background plasma as well as with stabilisation of the bursting MHD modes.
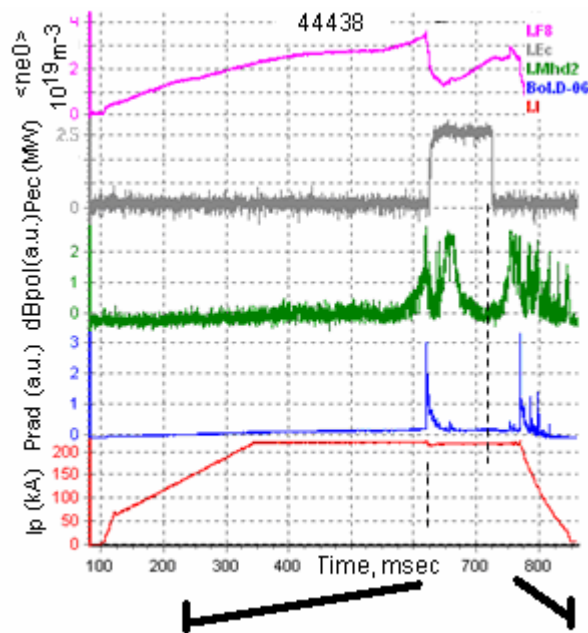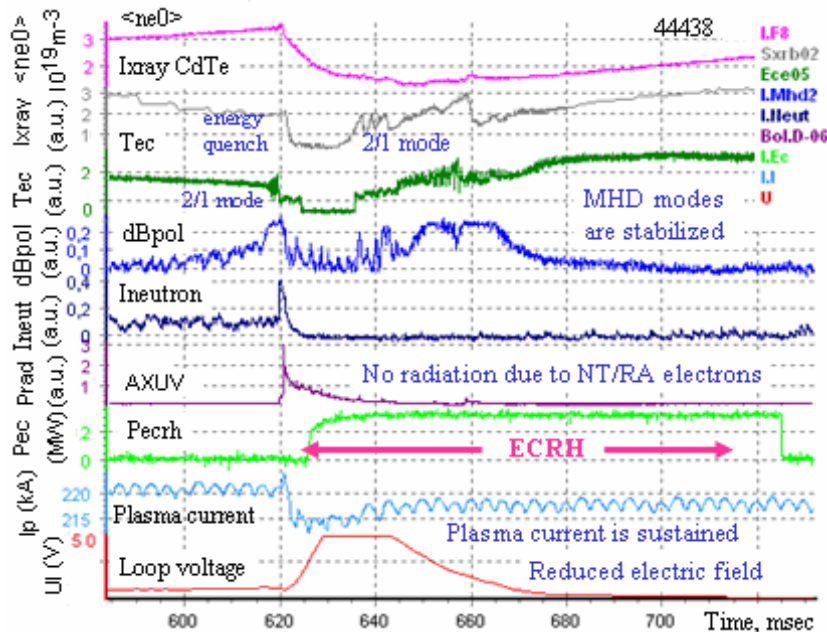
Acknowledgements

FIG. 6 *(a) Time evolution of the electron density <ne0>, ECRH power Pecrh, poloidal magnetic field perturbations dBpol, total radiation measured using AXUV detector Prad, and plasma current Ip during density limit disruption in plasma with ECRH heating (total heating power of up to 2.5MW: 1.2MW at 130 GHz and 1.3MWat 140 GHz). ECRH power is switched on at t=625msec (5 msec after the energy quench). The bursting MHD modes and the radiation bursts (see P_{bol}) connected with the nonthermal electrons are eliminated during whole duration of the ECRH pulse.*

(b) Expanded view of time evolution of the electron density <ne0>, soft x-ray intensity measured using CdTe detector SXRB0 Ixray, ECE electron temperature Tec, poloidal magnetic field perturbations dBpol, neutron radiation Ineutr, total radiation measured using AXUV detector Prad, ECRH power Pec, plasma current Ip, and loop voltage Ul during density limit disruption.

References:

[1] ITER Physics Expert Group on Disruptions, Plasma Control, and MHD, ITER Physics Basis Editors, Nucl. Fusion 39, (1999) 2251.

[2] R.Yoshino, et al., Nucl. Fusion 40, 1293 (2000).

[3] SAVRUKHIN, P. V., Phys. Rev. Lett. 86, 3036 (2001).

[4] P.V.Savrukhin, et al., Nucl. Fusion 34 (1994) 317.

[5] A.V.Sushkov, Rev.Sci.Instrum. (2008) to be published

[6] D.V.Sarychev, Rev.Sci.Instrum. (2008) to be published

[7] BISKAMP, D., Nonlinear magnetohydrodynamic, Cambridge University Press, Cambridge (1993).

[8] P.V.Savrukhin. Physics of Plasmas, 9 (2002) 3421.

[9] R.D.Gill, Nucl. Fusion 40 (2000) 163.

[10] FREDRICKSON, E. D., et al., Physics of Plasmas 3, (1996) 2620.

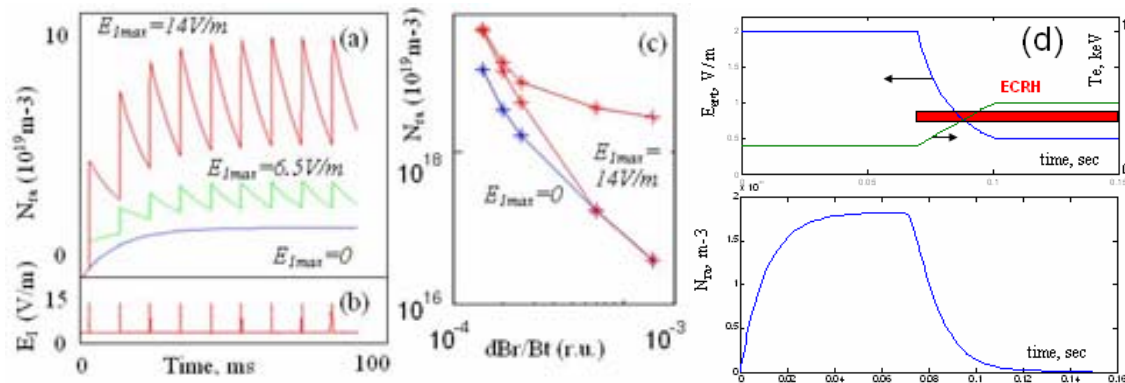[11] V.V.Plyusnin, et al., Nucl. Fusion 46 (2006) 277.

FIG. 7. Numerical modeling of the runaway beams in the T-10 plasma. (a)Temporal evolution of the runaway beam density in presence of standard quasi-static electric field (E_0=2V/m) superimposed with repetitive bursts of the electric fields (E_1) induced during periodic reconnection. Three curves represent results of the simulations for E_1max=0, 6.5V/m, and 14V/m. (b) Temporal evolution of the electric fields (E_1) for the case E_1max=14V/m. (c) Runaway beam density N_{ra} in plasma with various amplitude of the magnetic perturbations (B_r/B_t) for two values of the induced electric fields: E_1max=0 and E_1max=14V/m. (d) Numerical modeling of the runaway beams in the T-10 plasma with ECRH heating. Runaway beam density N_{ra} is decreased in plasma with increased electron temperature and reduced longitudinal electric field.